JPET Fast Forward. Published on November 3, 2004 as DOI: 10.1124/jpet.104.079707

Title: Ethyl pyruvate inhibits NF-κB-dependent signaling by directly targeting p65*

Authors: Yusheng Han, Joshua A. Englert, Runkuan Yang, Russell L. Delude, Mitchell P. Fink

Institution: Departments of Critical Care Medicine (Y.H., J.A., R.Y., R.L.D., M.P.F.), Pathology (R.L.D.), and Surgery (M.P.F.), University of Pittsburgh School of Medicine, Pittsburgh, PA, 15261

Running Title: Ethyl pyruvate inhibits KF-κB

Correspondence: Mitchell P. Fink, M.D.

Department of Critical Care Medicine

615 Scaife Hall, 3550 Terrace Street

Pittsburgh, PA 15261

Tel: (412) 647-6965

Fax: (412) 647-5258

email: finkmp@ccm.upmc.edu

number of text pages: 32

tables: 0

figures: 11

words in the *Abstract*: 226

words in the *Introduction*: 571

words in the *Discussion*: 1182

Abbreviations:

Cys^{38}, cysteine 38 to serine (Cys→Ser) mutant p65; Cys^{120}, cysteine 120 to alanine (Cys→Ala) mutant p65; EMSA, electrophoretic mobility shift assay; IKK, IκB kinase; iNOS; inducible nitric oxide synthase; NF-κB, nuclear factor-κB; NF-IL6, nuclear factor-interleukin 6; NP-40, Nonidet P-40; RT-PCR, reverse transcriptase - polymerase chain reaction; ROS, reactive oxygen species

Section assignment: Inflammation and Immunopharmacology

JPET Fast Forward. Published on November 3, 2004 as DOI: 10.1124/jpet.104.079707
This article has not been copyedited and formatted. The final version may differ from this version.

ABSTRACT

Ethyl pyruvate has been shown to have anti-inflammatory properties in numerous cell culture and animal studies. In this series of experiments, we tested the hypothesis that ethyl pyruvate inhibits signaling by the pro-inflammatory transcription factor, NF-κB. Ethyl pyruvate inhibited luciferase expression in lipopolysaccharide-stimulated murine macrophage-like RAW 264.7 cells transfected with an NF-κB-dependent luciferase reporter vector. ethyl pyruvate also decreased NF-κB DNA-binding activity in lipopolysaccharide-stimulated RAW 264.7 cells and decreased lipopolysaccharide-induced expression of an NF-κB-dependent gene, inducible nitric oxide synthase. Ethyl pyruvate had no effect on the degradation of IκBα or IκBβ in lipopolysaccharide-stimulated RAW 264.7 cells, suggesting that ethyl pyruvate acts distally to this step in the activation of NF-κB. In a cell-free system, binding of p50 homodimers to an NF-κB consensus oligonucleotide sequence was unaffected by ethyl pyruvate over a wide range of concentrations, indicating that ethyl pyruvate probably does not modify or interact with the p50 subunit of NF-κB. In contrast, ethyl pyruvate inhibited DNA binding by ectopically overexpressed wild-type p65 homodimers. However, ethyl pyruvate failed to inhibit the DNA-binding activity of homodimers of an overexpressed mutant form of a p65 with substitution of serine for cysteine 38. Taken together, these results suggest that ethyl pyruvate inhibits DNA-binding by covalently modifying p65 at Cys^{38}. We conclude that some of the beneficial anti-inflammatory effects of ethyl pyruvate may be due to modification of p65, thereby inhibiting signaling via the NF-κB pathway.

Ethyl pyruvate is a simple aliphatic ester derived from the endogenous metabolite, pyruvic acid. In previous studies performed by our laboratory and others, ethyl pyruvate has been shown to ameliorate intestinal, renal or hepatic injury when it is used as a therapeutic agent to treat rodents subjected to mesenteric ischemia and reperfusion (Sims et al., 2001;Uchiyama et al., 2003), hemorrhagic shock (Tawadrous et al., 2002;Yang et al., 2002), endotoxemia (Ulloa et al., 2002;Venkataraman et al., 2002), or polymicrobial bacterial sepsis (Ulloa et al., 2002;Miyaji et al., 2003). Treatment with ethyl pyruvate also ameliorates organ dysfunction in murine models of acute pancreatitis (Yang et al., 2004) and alcoholic hepatitis (Yang et al., 2003). In many of these models of acute critical illness, treatment with ethyl pyruvate down-regulates the expression of various pro-inflammatory genes, including inducible nitric oxide synthase (iNOS), tumor necrosis factor (TNF), cyclooxygenase-2, and interleukin (IL)-6 (Yang et al., 2004;Yang et al., 2003;Yang et al., 2002;Uchiyama et al., 2003). Similarly, ethyl pyruvate inhibits IL-6 and iNOS expression, nitric oxide production, and/or secretion of the pro-inflammatory protein, HGMB1, by immunostimulated Caco-2 human enterocyte-like cells or lipopolysaccharide-stimulated RAW 264.7 murine macrophage-like cells (Sappington et al., 2003b; Sappington et al., 2003a; Song et al., 2004; Ulloa et al., 2002). These latter findings support the view that ethyl pyruvate has activity as an anti-inflammatory agent. However, the molecular mechanisms underlying the anti-inflammatory effects of ethyl pyruvate remain to be elucidated.

Nuclear factor-κB is the generic term for a family of transcription factors formed by the hetero- or homodimerization of proteins from the Rel family (Lawrence et al., 2001). There are five Rel proteins: p50, p65 (RelA), c-Rel, p52 and RelB (Senftleben and Karin, 2002). NF-κB is thought to play a pivotal role in immune and inflammatory responses through the regulation of

genes encoding pro-inflammatory cytokines, adhesion molecules, chemokines, growth factors and inducible enzymes, such as cyclooxygenase-2 and iNOS (Karin and Ben-Neriah, 2000;Tak and Firestein, 2001). In resting cells, the homo- or heterodimeric forms of NF-κB exist in the cytoplasm in an inactive form due to binding by a third inhibitory protein, called IκB (Baldwin, 1996). In mammalian cells, several IκB-like proteins have been identified: IκBα, IκBβ, IκBε, and Bcl-3 (Baldwin, 1996). Upon stimulation of the cell by a proinflammatory trigger—for example, cytokines like TNF or IL-1β or the bacterial product, lipopolysaccharide—IκB is phosphorylated on two key serine residues (Ser^{32} and Ser^{36} in IκBα), which targets the molecule for ubiquitination and subsequent proteasomal degradation (DiDonato et al., 1996). Phosphorylation of IκB is thought be mediated by an enzyme complex called IκB kinase (IKK) that contains two catalytic subunits, IKKα (IKK1) and IKKβ (IKK2) (Senftleben and Karin, 2002). Phosphorylation, release and degradation of IκB permits translocation of the transcriptionally competent form of NF-κB into the nucleus where it can bind to *cis*-acting elements in the promoter regions of various NF-κB-responsive genes.

Inspection of the predicted p65 primary sequence reveals nine cysteine residues that are exclusively clustered in the Rel homology/DNA binding domain of this protein. Six of these cysteine residues are highly conserved among all other known Rel-related proteins (Gilmore, 1990;Ruben et al., 1991). NF-κB DNA-binding activity *in vitro* is potently inhibited by a number of agents that oxidize or alkylate sulfhydryl residues (Toledano and Leonard, 1991; Toledano et al., 1993; Garcia-Pineres et al., 2001;Lyss et al., 1998).

Results from *in vivo* and *in vitro* studies support the view that ethyl pyruvate inhibits NF-κB DNA binding (Han et al., 2004; Song et al., 2004;Yang et al., 2004;Yang et al., 2003; Uchiyama et al., 2003;Yang et al., 2002). Moreover, Song et al. recently reported data,

suggesting that ethyl pyruvate might react with the sulfhydryl-containing compound, glutathione (Song et al., 2004). Prompted by these findings, we carried out a series of *in vitro* experiments designed to better elucidate the mechanisms responsible for inhibition of NF-κB-dependent signaling by ethyl pyruvate. Specifically, we sought to test the hypothesis that the anti-inflammatory effects of ethyl pyruvate are due, at least in part, to modification of key thiol residues in one or more of the proteins involved in the formation of transcriptionally active NF-κB dimers.

MATERIALS AND METHODS

Materials. All chemicals were purchased from Sigma-Aldrich Chemical Co. (St. Louis, MO) unless otherwise noted. Human recombinant purified p50 protein was purchased from Promega (Madison, WI). The mammalian expression vectors containing wild-type p65, cysteine 38 to serine (Cys→Ser) mutant p65 (Cys^{38}), cysteine 120 to alanine (Cys→Ala) mutant p65 (Cys^{120}), and the empty control vector (pRc/CMV) were generous gifts from Dr. Irmgard Merfort (Institute of Pharmaceutical Biology, Albert-Ludwigs-Universität, Freiburg, Germany).

Cell culture. The murine macrophage-like RAW 264.7 and human embryonic kidney 293 cell lines were obtained from the American Type Culture Collection (Rockville, MD). RAW 264.7 cells were maintained in RPMI 1640 medium and 293 cells were maintained in Dulbecco's modified Eagle's medium. Both media were supplemented with 10% heat-inactivated fetal bovine serum (Hyclone, Logan, UT), 100 IU/ml penicillin, and 100 μg/ml streptomycin. Cells were grown at 37 ºC in a humidified atmosphere containing 8% CO_2 and 92% air.

NF-κB reporter gene transfection and analysis. In order to measure the effects if ethyl pyruvate on NF-κB *trans*-activating activity, we employed an NF-κB reporter construct (pNF-κB-luc) containing four tandem copies of the κ light chain gene enhancer element fused to a herpes simplex virus minimal promoter directing expression of a luciferase reporter gene (BD Biosciences, Clontech, Palo Alto, CA). RAW 264.7 cells were plated in 6-well plates at a density of 8.5×10^5 cells per well 12-16 h before transfection. The cells in each well were transfected with 2 μg of reporter plasmid and 0.4 μg of pSV-β-galactosidase vector (Promega)

using 6 μl of Lipofectamine 2000 reagent per well (Invitrogen, Carlsbad, CA) as described by the manufacturer. After 24 h, the cells were exposed to the indicated concentration of ethyl pyruvate and incubated for 30 min before being exposed to *Escherichia coli* 0111:B4 lipopolysaccharide (100 ng/ml) for 30 min at 37 ºC. Luciferase activity in 20 μl of whole cell lysates was measured using the enhanced luciferase assay kit (BD Biosciences) and a Bio-Orbit 1250 luminometer (LKB-Wallac, Turku, Finland). Luciferase activity was normalized to β-galactosidase enzymatic activity measured by the cleavage of *o*-nitrophenyl β-D-galactopyranoside in whole cell extracts (Griffiths and Muir, 1978). Additionally, 293 cells were transfected with expression plasmids containing either wild-type p65, Cys^{38}/p65, or Cys^{120}/p65 using the method described above. All transfection experiments were carried out in triplicate and repeated separately at least three times.

Preparation of nuclear and cytosolic extracts. Cells were harvested and centrifuged at 1000 *g* for 5 min. The pellet was resuspended in 400 μl of buffer I [10 mM Tris, pH 7.8, 5 mM $MgCl_2$, 10 mM KCl, 0.3 mM EGTA, 0.5 mM dithiothreitol, 0.3 M sucrose, 1 mM phenylmethylsulfonyl fluoride, 1.0 mM sodium orthovanadate and 1× mammalian protease inhibitor cocktail (Sigma Catalog #P2714). The tubes were placed on ice for 15 min to allow the cells to swell and facilitate lysis. Nonidet P-40 (NP-40) was added to final concentration of 0.5% (v/v), and the tube were vortexed at full speed for 10 s. Nuclei were harvested by centrifugation at 7,200 g for 10 s at 4 °C. The supernatant was aspirated, and the nuclei were resuspended in 50 μl of buffer II (20 mM Tris, pH 7.8, 5 mM $MgCl_2$, 320 mM KCl, 0.2 EGTA, 0.5 mM dithiothreitol, and the mixture of protease inhibitors described above). Nuclear proteins were extracted for 15 min on ice followed by centrifugation at 13,500 g for 15 min. For experiments

with 293 cells transfected with wild-type or mutant p65 expression vectors, cytosolic extracts were prepared using buffer II supplemented with 1% NP-40 and incubated for 30 min on ice followed by centrifugation at 12,000 g for 5 min. Protein concentrations were determined using the Bio-Rad protein concentration reagent (Bio-Rad, Hercules, CA).

A denaturation/renaturation protocol was used to dissociate IκB from NF-κB in cytosolic extracts (Baeuerle and Baltimore, 1988a;Baeuerle and Baltimore, 1988b). RAW 264.7 cells were incubated in the absence or presence of graded concentrations of ethyl pyruvate for 1 h. The cells were lysed using buffer I and NP-40 as described for making nuclear extracts above. The cytosolic fraction was dialyzed against 10,000 volumes of buffer II. Sodium deoxycholate [0.2% (w/v) final concentration) was added to 5 μg of cytosolic protein and incubated on ice for 15 min. NP-40 (0.2% v/v final concentration) was added to the solution, which was incubated for an additional 15 min on ice before being analyzed using the electrophoretic mobility shift assay (EMSA). This sequential treatment effectively removes IκB from NF-κB, allowing the detection of total NF-κB DNA-binding activity present in the cytosol of resting cells.

Electrophoretic mobility shift assay (EMSA). The EMSA used to measure DNA-binding activity was carried out using a double stranded oligonucleotide, as previously published (Delude et al., 1994). Briefly, the sequence of the double-stranded NF-κB oligonucleotide was as follows: sense, 5′-AGT TGA GGG GAC TTT CCC AGG C-3′; antisense, 3′-TCA ACT CCC CTG AAA GGG TCC G-5′ (NF-κB DNA binding consensus sequence is underlined; Promega). The oligonucleotides were end-labeled with γ-[^{32}P]-ATP (PerkinElmer Life and Analytical Sciences, Inc.; Boston, MA) using T4 polynucleotide kinase (Promega). 3 μg of nuclear protein/reaction or 10 μg total cellular protein were incubated with radiolabeled NF-κB probe in bandshift buffer

(10 mM Tris, pH 7.8, 40 mM KCl, and 1 mM EDTA) in the presence of 2 μg of poly (dI·dC) for 20 min at room temperature. The binding reaction mixture was electrophoresed on 4% non-denaturing polyacrylamide gels, which were then dried and used to expose Kodak X-omat AR film (Rochester, NY) at –80 °C overnight using an intensifying screen.

To determine the specificity of DNA/protein complexes observed in the EMSA, we carried out "cold competition" studies using a 100-fold molar excess of either unlabeled NF-κB duplex oligonucleotide (specific competition) or a 100-fold molar excess of an irrelevant oligonucleotide (nonspecific competition). The irrelevant oligonucleotide contained the murine NF-IL6 consensus sequence (upper 5'- CTG CCG CTG CGG TTC TTG CGC AAC TCA CT -3'; lower 5'- AGT GAG TTG CGC AAG AAC CGC AGC GGC AG -3'; NF-IL6 DNA binding consensus sequence is underlined; Gibco-BRL, Gaithersburg, MD). Supershift assays were performed by pre-incubating the nuclear extracts with 2 μl of anti-p65 and anti-p50 antibodies (Santa Cruz Biotechnology, Santa Cruz, CA) for 1 h at room temperature before the addition of the radiolabeled probe. The binding reaction mixture was electrophoresed on 4% PAGE gels.

In vitro experiments with human recombinant p50. Human recombinant p50 was dissolved in buffer containing 20 mM Tris, pH 7.5, 50 mM NaCl, 5 mM $MgCl_2$, 1 mM EDTA, 0.7 μM 2-mercaptoethanol, 5% glycerol and 0.01% NP-40. 11 ng of p50 were incubated with ethyl pyruvate or vehicle for 2 h at 37 °C before being analyzed by EMSA.

Reverse transcription polymerase chain reaction (RT-PCR). Total RNA was extracted from harvested cells with chloroform and TRI reagent (Molecular Research Center, Cincinnati, OH) exactly as directed by the manufacturer. We treated the total RNA with DNAFree (Ambion,

Houston, TX) as instructed by the manufacturer, using 10 U DNase I/10 µg RNA. Two micrograms of total RNA were reverse transcribed in a 40-µl reaction volume containing 0.5 µg oligo$(dT)_{15}$ (Promega), 1 mM of each dNTP, 15 units avian myeloblastosis virus RT (Promega), and 1 U/µl recombinant RNasin ribonuclease inhibitor (Promega) in 5 mM MgCl2, 10 mM Tris, pH 8.0, 50 mM KCl, and 0.1% Triton X-100. The reaction mixtures were preincubated at 21 °C for 10 min before DNA synthesis. The RT reactions were carried out for 50 min at 42 °C and were heated to 95 °C for 5 min to terminate the reaction. Reaction mixtures (50 µl) for PCR were assembled using 5 µl cDNA template, 10 units AdvanTaq Plus DNA polymerase (Clontech, Palo Alto, CA), 200 µM of each dNTP, 1.5 mM $MgCl_2$, and 1.0 µM of each primer in 1× AdvanTaq Plus PCR buffer. Amplification of cDNA for iNOS was carried out by denaturing at 94 °C for 45 s, annealing at 58 °C for 1 min, and polymerizing at 72 °C for 45 s for 35 cycles. This number of PCR cycles was empirically determined to ensure that amplification was in the linear range. After the last cycle of amplification, the samples were incubated in 72 °C for 10 min and then held at 4 °C. The 5' and 3' primers for iNOS were CAC CAC AAG GCC ACA TCG GAT T and CCG ACC TGA TGT TGC CAT TGT T, respectively (Invitrogen, Carlsbad, CA); the expected product length was 426 bp. 18S ribosomal RNA was amplified to verify equal loading. For this reaction, the 5' and 3' primers were CCC GGG GAG GTA GTG ACG AAA AAT and CGC CCG CTC CCA AGA TCC AAC TAC, respectively; the expected product length was 200 bp. Ten µl of each PCR reaction was electrophoresed on a 2% agarose gel, scanned using a NucleoVision imaging workstation (NucleoTech, San Mateo, CA), and quantified using GelExpert release 3.5.

Western blotting. After washing with ice-cold PBS, cells were lysed in 1 ml of RIPA buffer, consisting of 1x PPS, 1% NP-40, 0.5% sodium deoxycholate, 0.1% SDS, 0.1 mg/ml phenylmethylsulfonyl fluoride, 1.0 mM sodium orthovanadate, and 1× mammalian protease inhibitor cocktail (Sigma-Aldrich Catalog # P8340). The cells were removed from the tissue culture plate and transferred to a 1.5 ml microfuge tube and incubated for 30 min on ice. The lysate was centrifuged at 12,000 *g* for 5 min at 4 °C. Protein concentrations were quantitated using the Bio-Rad assay. Equal amounts of total protein extract were mixed in 2× Laemmli buffer, boiled for 5 min, and centrifuged for 10 s. Proteins were resolved by electrophoresis on 4-15% precast gradient sodium dodecyl sulfate-PAGE (Bio-Rad), transferred to a Hybond-P polyvinylidene difluoride membrane (Amersham Pharmacia Biotech, Leicester, UK) and probed sequentially with antibody. The filter was incubated at room temperature for 1 h with primary antibody diluted 1:2,000 in TBST (10 mM Tris, pH 7.5, 150 mM NaCl, 0.05% Tween 20). After being washed three times in TBST, immunoblots were exposed for 1 h to the appropriate horseradish peroxidase-conjugated secondary antibody. After three washes in TBST, the membrane was impregnated with the Enhanced Chemiluminescence substrate (Amersham Pharmacia Biotech) and used to expose X-ray film. The following antibodies were used: rabbit polyclonal anti-IκBα (Santa Cruz Biotechnology, Santa Cruz, CA), rabbit polyclonal anti-IκBβ (Santa Cruz Biotechnology) and rabbit polyclonal anti-iNOS (BD Bioscience).

Cell viability. Cell viability was assessed by determining exclusion of the vital dye, trypan blue. Briefly, cells exposed to ethyl pyruvate were incubated for 24 h before harvesting and incubating with trypan blue (final concentration 0.4%) for 5 min. Viability was assessed by determining the number of blue-stained cells per 100 total cells using light microscopy.

Statistical analysis. Data are presented as means ± SD. Statistical significance of differences among treatment conditions was assessed using one-way analysis of variance followed by Fisher's protected least significant difference post hoc testing procedure. Differences were considered to be statistically significant for $P<0.05$.

RESULTS

Ethyl pyruvate inhibits iNOS transcription and expression in lipopolysaccharide-stimulated RAW 264.7 cells. The iNOS gene in RAW 264.7 cells is regulated, at least in part, by activation of NF-κB (Kim et al., 1997). Therefore, we investigated the effect of ethyl pyruvate on lipopolysaccharide-induced iNOS expression in these cells. After pretreating RAW 264.7 cells with ethyl pyruvate for 30 min, we exposed them to lipopolysaccharide (100 ng/ml) for 24 h. Total RNA and total cellular proteins were prepared and then analyzed using RT-PCR and Western blotting, respectively. As shown in Figure 1, lipopolysaccharide-induced iNOS mRNA expression was suppressed by ethyl pyruvate in a dose-dependent manner. Similarly, lipopolysaccharide-induced iNOS protein expression was also inhibited by ethyl pyruvate (Figure 2).

Ethyl pyruvate inhibits NF-κB activation in lipopolysaccharide-stimulated RAW 264.7 cells. We employed RAW 264.7 murine macrophage-like cells transiently transfected with an NF-κB-responsive luciferase reporter gene. When these cells were incubated with 100 ng/ml lipopolysaccharide for 30 min, reporter activity increased by approximately 9-fold (Figure 3). Pretreatment of these cells with ethyl pyruvate inhibited this lipopolysaccharide-induced NF-κB reporter activity in a dose-dependent manner. Inhibition of NF-κB-dependent gene expression was significant when cells were incubated with 1 mM ethyl pyruvate and incubation of the cells with 10 mM ethyl pyruvate inhibited reporter activity by approximately 50%.

The ability of ethyl pyruvate to inhibit lipopolysaccharide-induced NF-κB transcriptional activity was further confirmed by EMSA. RAW 264.7 cells were pre-incubated with graded concentrations of ethyl pyruvate for 30 min, and then exposed to lipopolysaccharide (100 ng/ml)

for 15 min. Nuclear extracts were prepared and EMSA performed. As shown in Figure 4, 10 mM ethyl pyruvate clearly decreased NF-κB DNA binding. Pre-incubation of the cells with 20 mM ethyl pyruvate almost completely blocked the increase in NF-κB DNA binding induced by lipopolysaccharide.

Ethyl pyruvate fails to inhibit degradation of IκBα and IκBβ in lipopolysaccharide-stimulated RAW 264.7 cells. The activation of NF-κB requires phosphorylation of the IκB subunit by IκB kinase and subsequent proteasomal degradation of IκB (Senftleben and Karin, 2002). Thus, one way that ethyl pyruvate might inhibit NF-κB activation is by blocking one or more proximal steps in the activation pathway, and thereby preventing degradation of IκB. In order to test this hypothesis, we assessed the effect of graded concentrations of ethyl pyruvate on lipopolysaccharide-induced degradation of IκBα and IκBβ. In preliminary studies, we found that the greatest decrease in IκBα and IκBβ protein levels was evident when RAW 264.7 cells were incubated with lipopolysaccharide (100 ng/ml) for 1 h (data not shown). Accordingly, to elucidate the effect of ethyl pyruvate on lipopolysaccharide-induced degradation of IκBα and IκBβ, we pretreated RAW 264.7 cells with graded concentrations of ethyl pyruvate for 30 min, and then added lipopolysaccharide (100 ng/ml) for 1 h. As shown in Figure 5, ethyl pyruvate over a wide range of concentrations had no effect at all on lipopolysaccharide-induced IκBα or IκBβ degradation. Thus, inhibition of IκB degradation does not appear to be responsible for blocking activation of NF-κB.

Ethyl pyruvate inhibits DNA binding by detergent-activated NF-κB. We hypothesized that ethyl pyruvate inhibits NF-κB by covalently modifying one or more critical thiol groups required for DNA-binding activity. In order to test this hypothesis, we first demonstrated that ethyl pyruvate inhibited basal NF-κB DNA-binding activity present in nuclear extracts prepared from unstimulated cells in a concentration-dependent fashion (Figure 6). This finding is consistent with the view that at least some of the effects of ethyl pyruvate on NF-κB-dependent signaling are independent of the cascade of events that are initiated by binding of lipopolysaccharide to its transmembrane receptor. In order to confirm this possibility, we took advantage of the observation that treating cytoplasmic extracts with deoxycholate followed by NP-40 effectively dissociates heterodimeric complexes of NF-κB from their inhibitory subunits (e.g., IκB), allowing NF-κB to bind specifically to DNA probes *in vitro* (Baeuerle and Baltimore, 1988a). Cytosolic extracts were prepared from untreated RAW 264.7 cells or cells that had been treated with 10 mM ethyl pyruvate for 1 h. The extracts were treated with deoxycholate and NP-40 and then analyzed by EMSA. Deoxycholate/NP-40 treatment of cytosolic extracts from cells that had not been treated with ethyl pyruvate revealed the presence of significant quantities of NF-κB DNA binding activity (Figure 7). In contrast, specific binding to an NF-κB probe was markedly decreased in detergent-activated cytoplasmic extracts prepared from RAW 264.7 cells treated with 10 mM ethyl pyruvate for 1 h. Western blotting showed that treatment with ethyl pyruvate did not decrease total cellular levels of either p50 or p65 (data not shown). Taken together, these findings support the view that ethyl pyruvate may lead to a modification of the NF-κB proteins p65 or p50 or both in such a way that DNA binding is inhibited.

Ethyl pyruvate fails inhibit DNA binding by human recombinant p50 homodimers in a cell-free system. We speculated that p50 might be the target for ethyl pyruvate in the NF-κB complex. In order to test this hypothesis, we took advantage of the fact that p50 spontaneously forms homodimers that are capable of binding to NF-κB DNA motifs. Accordingly, we carried out experiments, wherein recombinant human p50 was pre-incubated with graded concentrations of ethyl pyruvate in a cell-free system (Figure 8). The results showed that the ability of p50 to bind to the κB consensus sequence was not inhibited by ethyl pyruvate over a range of concentrations from 1 to 40 mM. These data support the view that ethyl pyruvate has no effect on DNA binding of the NF-κB p50 subunit.

Ethyl pyruvate impairs DNA binding by p65 homodimers in 293 cells. When high levels of p65 are expressed in cells, homodimers form spontaneously and these dimers are capable of binding to κB DNA sequences (Ganchi et al., 1993). Therefore, to further investigate the effect of ethyl pyruvate on DNA-binding by the p65 subunit, we transfected 293 cells with a wt-p65 plasmid. Cells overexpressing wt-p65 were treated with graded concentrations of ethyl pyruvate for 4 h after which nuclear extracts were analyzed by EMSA. Although ethyl pyruvate clearly inhibited DNA binding by p65 homodimers (Figure 9), relatively high concentrations of the compound (≥30 mM) and a longer incubation time (120 min instead of 60 min, as in Figure 4) were required. We speculate that relatively higher concentrations of ethyl pyruvate and longer incubation time were needed to observe inhibition of DNA binding in this assay system, because of the very high level of expression of p65 in cells transfected with the wt-p65 plasmid.

It has been proposed that certain sesquiterpene lactones, which can form Michael-type adducts with sulfhydryl groups, can react with two key cysteine residues, Cys^{38} and Cys^{120}, in the

p65 molecule (Rungeler et al., 1999). Subsequently, however, it was shown that Cys^{38} is the primary target for parthenolide and related sesquiterpene lactones that are capable of inhibiting NF-κB-dependent transcription (Garcia-Pineres et al., 2001). Accordingly, we speculated that covalent modification of Cys^{38} and/or Cys^{120} in p65 might account for inhibition of DNA binding of p65 homodimers when cells are incubated with ethyl pyruvate. Therefore, we employed the Cys^{38} and Cys^{120} mutant plasmids described above to transiently transfect 293 cells. Transfected cells expressing the mutant proteins were incubated with graded concentrations of ethyl pyruvate, and DNA binding of cellular extracts was assessed using an EMSA. If ethyl pyruvate inhibited DNA binding by alkylating Cys^{38} or Cys^{120} or both, concentrations of the drug that completely inhibited binding in cells over-expressing wt-p65 should not affect binding in cells expressing the mutant proteins. In contrast to the results obtained with cells transfected with the wt-p65 plasmid, ethyl pyruvate had no effect on the DNA binding activity of p65 homodimers from cells transfected with the Cys^{38} mutant plasmid, even when the concentration of the drug was as high as 40 mM (Figure 10). However, DNA binding of p65 homodimers in cells expressing the Cys^{120} mutant p65 was inhibited by ethyl pyruvate at the same concentrations as those observed in cells transfected with the wt-p65 plasmid (Figure 11). These data support the view that Cys^{120} is not critical for the effect of ethyl pyruvate on p65 DNA binding. Cys^{38}, in contrast, appears to be critical for the ability of ethyl pyruvate to inhibit p65 DNA binding.

DISCUSSION

The data presented herein support the view that ethyl pyruvate at concentrations as low as 10 mM inhibits lipopolysaccharide-induced NF-κB activation in lipopolysaccharide-stimulated RAW 264.7 murine macrophage-like cells. Importantly, we used EMSA to show that ethyl pyruvate inhibits NF-κB DNA binding and we employed a luciferase reporter gene to document that ethyl pyruvate inhibits NF-κB-dependent gene transcription. Furthermore, we showed that ethyl pyruvate inhibits lipopolysaccharide-induced expression of an NF-κB dependent gene (iNOS).

The predominant form of NF-κB consists of p50 and p65 subunits that are sequestered in the cytoplasm of unstimulated cells by the inhibitory proteins, IκBα and IκBβ (Senftleben and Karin, 2002). Phosphorylation and rapid degradation of IκBα and IκBβ allows p50/p60 heterodimers to translocate into the nucleus and bind to target genes. A wide variety of pharmacological agents that are known to inhibit NF-κB-dependent signal transduction, do so, at least in part, by blocking IκB phosphorylation/degradation. These compounds include: the polyphenolic glycoside, oleandrin (Manna et al., 2000); the antirheumatic gold compound, auranofin (Jeon et al., 2000); the endogenous anti-oxidant, vitamin C (Bowie and O'Neill, 2000); and the naturally occuring chain-breaking anti-oxidant, curcumin (Brennan and O'Neill, 1998). Although ethyl pyruvate clearly inhibited NF-κB DNA binding and NF-κB-dependent gene transcription, treatment of RAW 264.7 cells with this compound had no effect whatsoever on lipopolysaccharide-induced IκBα or IκBβ degradation. Other anti-inflammatory agents are known to inhibit NF-κB DNA binding and NF-κB-mediated signaling at a step distal to IκB phosphorylation/degradation. Compounds in this category include: the anti-oxidant flavonoid, caffeic acid phenethyl ester (Natarajan et al., 1996); the anti-inflammatory sesquiterpene lactone,

helanin (Lyss et al., 1998); and, the anti-psoriatic agent, dimethylfumarate (Loewe et al., 2002). The last named compound is particularly interesting in the context of the present series of experiments because dimethylfumarate, like ethyl pyruvate, is a simple aliphatic ester of an α-keto carboxylic acid.

Ethyl pyruvate inhibited basal DNA binding of NF-κB in unstimulated RAW 264.7 cells. This observation suggests that ethyl pyruvate does not act by interfering with steps involved in the activation of the NF-κB pathway, but rather directly interferes with DNA binding NF-κB dimers, possibly by covalently modifying one or more of the subunit proteins. To further investigate this notion, we took advantage of previously published work by Baeuerle and co-workers, who showed that sequential treatment of cytosolic extracts with deoxycholate and Nonidet P-40 leads to chemical dissociation of IκB from the transcriptionally active NF-κB complex (Baeuerle and Baltimore, 1988a). Herein, we showed that treatment of cells with ethyl pyruvate prior to preparing cytosolic extracts interfered with DNA binding by detergent-activated NF-κB. Thus, ethyl pyruvate must inhibit NF-κB DNA binding at a step distal to the freeing of transcriptionally active dimers from the interaction with IκB proteins.

The Rel homology domain of p65 has been shown to mediate multiple biological functions of this particular transcription factor, including its interaction with DNA enhancer elements, IκB, and other Rel protein family members (Ballard et al., 1992; Beg et al., 1992; Ganchi et al., 1992; Schmitz and Baeuerle, 1991). Biochemical studies with purified p65 suggest that this NF-κB subunit engages its cognate enhancer as a homodimer, presumably reflecting a requirement for the apposition of certain key amino acids from each monomer to form a functional DNA binding domain (Ganchi et al., 1993). When cells were transfected with a plasmid encoding wt-p65, we observed DNA binding by spontaneously formed p65 homodimers. DNA binding by these

homodimers was inhibited by ethyl pyruvate in a concentration-dependent fashion. It is known that cysteine 38 in the p65 subunit of NF-κB participates in DNA binding by forming a hydrogen bond with the phosphate backbone of the κB-DNA motif (Berkowitz et al., 2002). Data have been presented previously to support the view that alkylation of cysteine 38 in p65 inhibits NF-κB DNA binding by steric hindrance of protein binding to the DNA (Garcia-Pineres et al., 2001). Based on *in silico* molecular modeling studies of NF-κB homo- and heterodimers (Chen et al., 2003; Huxford et al., 1998; Chen et al., 1998a; Chen et al., 1998b)(data not shown), it is apparent that cysteine 38 is exposed (to the solvent) on the surface of p65. Thus, we believe that it is unlikely that covalent modification of cysteine 38 by ethyl pyruvate would interfere with either homo- or heterodimerization of p50 or p65s subunits. It is noteworthy, therefore, that DNA binding by the Cys^{38} mutant was unaffected by a concentrations of ethyl pyruvate higher than those that completely blocked DNA binding by wt-p65 homodimers. In contrast, DNA binding by the Cys^{120} mutant was inhibited by the same concentrations of ethyl pyruvate as were required to preventing DNA binding by the wt-p65 homodimer. Finally, DNA binding by spontaneously formed p50 homodimers was unaffected by ethyl pyruvate, even when the protein was incubated with high concentrations of the ester. Collectively, these observations support the view that ethyl pyruvate interferes with NF-κB-dependent signaling by modifying p65 at cysteine 38.

Interestingly, p50 lacks a transcription activation domain (Schmitz et al., 1995). Furthermore, p50 homodimers can repress transcription of proinflammatory genes (Baer et al., 1998). Thus, ethyl pyruvate-dependent modification of p65 but not p50 would be expected to decrease NF-κB-dependent activation of proinflammatory gene expression, while preserving the antiinflammatory potential of p50 homodimers.

A relatively high concentration of ethyl pyruvate (≥30 mM) was required to inhibit DNA binding by wt-p65 homodimers. These concentrations of ethyl pyruvate were higher than those required to inhibit lipopolysaccharide-induced NF-κB activation in RAW 264.7 cells. Presumably, relatively higher concentrations of ethyl pyruvate were required to inhibit DNA binding by wt-65 homodimers in cytosolic extracts from transfected 293 cells, because these cells were expressing much higher levels of the protein than were present in stimulated RAW 264.7 cells.

It is well known that pyruvic acid, a compound that is closely related to ethyl pyruvate, is an effective scavenger of the reactive oxygen species (ROS), hydrogen peroxide (Bunton, 1949;O'Donnell-Tormey et al., 1987). We have shown that pyruvate and ethyl pyruvate react similarly rapidly with hydrogen peroxide (Englert JA, Delude RL, Fink MP. Unpublished observations) and we have presented evidence to support the view that ethyl pyruvate inhibits lipid peroxidation, a marker of oxidant stress, *in vitro* (Song et al., 2004) and *in vivo* (Tawadrous et al., 2002). Thus, the activity of ethyl pyruvate as an ROS scavenger might account for its anti-inflammatory properties, since other ROS scavengers, such as N-acetylcysteine, are known to inhibit expression pro-inflammatory genes, at least under some conditions (Song et al., 2004). This notion, however, is not supported by observations recently reported by Sappington et al., who showed that transient exposure to ethyl pyruvate inhibits iNOS expression in immunostimulated Caco-2 human enterocyte-like cells, even when the compound is removed from the culture medium by thorough washing of the cells (Sappington et al., 2003a). In contrast to the ROS scavenging hypothesis, which seems incompatible with the data obtained by Sappington and co-workers (Sappington et al., 2003a), covalent modification of the p65 subunit of NF-κB, as suggested by the findings reported herein, is entirely compatible with the

observation that transient incubation with ethyl pyruvate provides a durable anti-inflammatory effect even in the absence of ongoing exposure to the compound.

In summary, our data support the view that ethyl pyruvate inhibits NF-κB signaling by directly targeting the p65 subunit of the transcription factor. As alluded to above, ethyl pyruvate also has been shown to have other pharmacological activities, including inhibition of p38 activation (Ulloa et al., 2002) and lipid peroxidation (Song et al., 2004), that might be beneficial under conditions associated with excessive inflammation. Therefore, further studies will be required to determine whether inhibition of NF-κB-dependent gene transcription is the primary basis for the beneficial effects of ethyl pyruvate observed in numerous studies of this compound in pre-clinical models of critical illness. Nevertheless, the results presented herein provide a better understanding of the molecular pharmacology of the simple ester, ethyl pyruvate.

Acknowledgements

The authors thank Ms. Meaghan E. Killeen and Ms. Angel L. Shaufl for their excellent technical assistance. Joshua A. Englert is a Howard Hughes Medical Institute Medical Student Research Fellow.

REFERENCES

Baer M, Dillner A, Schwartz RC, Sedon C, Nedospasov S, and Johnson PF (1998) Tumor necrosis factor alpha transcription in macrophages is attenuated by an autocrine factor that preferentially induces NF-kappaB p50. *Mol Cell Biol* **18**:5678-5689.

Baeuerle PA and Baltimore D (1988a) Activation of DNA-binding activity in an apparently cytoplasmic precursor of the NF-kappa B transcription factor. *Cell* **53**:211-217.

Baeuerle PA and Baltimore D (1988b) IkB: a specific inhibitor of the NF-kappaB transcription factor. *Science* **242**:540-546.

Baldwin AS (1996) The NF-kappaB and I kappa B proteins: new discoveries and new insights. *Annu Rev Immunol* **14**:649-683.

Ballard DW, Dixon EP, Peffer NJ, Bogerd H, Doerre S, Stein B, and Greene WC (1992) The 65-kDa subunit of human NF-kappa B functions as a potent transcriptional activator and a target for v-Rel-mediated repression. *Proc Natl Acad Sci USA* **89**:1875-1879.

Beg AA, Ruben SM, Scheinman RI, Haskill S, Rosen CA, and Baldwin AS, Jr. (1992) I kappa B interacts with the nuclear localization sequences of the subunits of NF-kappa B: a mechanism for cytoplasmic retention. *Genes Dev* **6**:1899-1913.

Berkowitz B, Huang DB, Chen-Park FE, Sigler PB, and Ghosh G (2002) The x-ray crystal structure of the NF-kappa B p50.p65 heterodimer bound to the interferon beta -kappa B site. *J Biol Chem* **277**:24694-24700.

Bowie AG and O'Neill LA (2000) Vitamin C inhibits NF-kappa B activation by TNF via the activation of p38 mitogen-activated protein kinase. *J Immunol* **165**:7180-7188.

Brennan P and O'Neill LA (1998) Inhibition of nuclear factor kappaB by direct modification in whole cells--mechanism of action of nordihydroguaiaritic acid, curcumin and thiol modifiers. *Biochem Pharmacol* **55**:965-973.

Bunton CA (1949) Oxidation of α-diketones and α-keto-acids by hydrogen peroxide. *Nature* **163**:144.

Chen FE, Huang DB, Chen YQ, and Ghosh G (1998a) Crystal structure of p50/p65 heterodimer of transcription factor NF-kappaB bound to DNA. *Nature* **391**:410-413.

Chen J, Anderson JB, DeWeese-Scott C, Fedorova ND, Geer LY, He S, Hurwitz DI, Jackson JD, Jacobs AR, Lanczycki CJ, Liebert CA, Liu C, Madej T, Marchler-Bauer A, Marchler GH, Mazumder R, Nikolskaya AN, Rao BS, Panchenko AR, Shoemaker BA, Simonyan V, Song JS, Thiessen PA, Vasudevan S, Wang Y, Yamashita RA, Yin JJ, and Bryant SH (2003) MMDB: Entrez's 3D-structure database. *Nucleic Acids Res* **31**:474-477.

Chen YQ, Ghosh S, and Ghosh G (1998b) A novel DNA recognition mode by the NF-kappa B p65 homodimer. *Nat Struct Biol* **5**:67-73.

Delude RL, Fenton MJ, Savedra RJr, Perera PY, Vogel SN, Thieringer R, and Golenbock DT (1994) CD14-mediated translocation of nuclear factor-kappa B induced by lipopolysaccharide does not require tyrosine kinase activity. *J Biol Chem* **269**:22253-22260.

DiDonato J, Mercurio F, Rosette C, Wu-Li J, Suyang H, Ghosh S, and Karin M (1996) Mapping of the inducible IkappaB phosphorylation sites that signal its ubiquitination and degradation. *Mol Cell Biol* **16**:1295-1304.

Ganchi PA, Sun SC, Greene WC, and Ballard DW (1992) I kappa B/MAD-3 masks the nuclear localization signal of NF-kappa B p65 and requires the transactivation domain to inhibit NF-kappa B p65 DNA binding. *Mol Biol Cell* **3**:1339-1352.

Ganchi PA, Sun SC, Greene WC, and Ballard DW (1993) A novel NF-kappa B complex containing p65 homodimers: implications for transcriptional control at the level of subunit dimerization. *Mol Cell Biol* **13**:7826-7835.

Garcia-Pineres AJ, Castro V, Mora G, Schmidt TJ, Strunk E, Pahl HL, and Merfort I (2001) Cysteine 38 in p65/NF-kappaB plays a crucial role in DNA binding inhibition by sesquiterpene lactones. *J Biol Chem* **276**:39713-39720.

Gilmore TD (1990) NF-kappa B, KBF1, dorsal, and related matters. *Cell* **62**:841-843.

Griffiths MW and Muir DD (1978) Properties of a thermostable β-galactosidase from a thermophilic Bacillus: comparison of the enzyme activity of whole cells, purified enzyme and immobilised whole cells. *J Sci Food Agric* **29**:753-761.

Han X, Fink MP, Uchiyama T, and Delude RL (2004) Increased iNOS activity is essential for the development of pulmonary epithelial tight junction dysfunction in endotoxemic mice. Am J Physiol Lung Cell Mol Physiol. *Am J Physiol Lung Cell Mol Physiol* **286**:L259-L267.

Huxford T, Huang DB, Malek S, and Ghosh G (1998) The crystal structure of the IkappaBalpha/NF-kappaB complex reveals mechanisms of NF-kappaB inactivation. *Cell* **95**:759-770.

Jeon KI, Jeong JY, and Jue DM (2000) Thiol-reactive metal compounds inhibit NF-kappa B activation by blocking I kappa B kinase. *J Immunol* **164**:5981-5989.

Karin M and Ben-Neriah Y (2000) Phosphorylation meets ubiquitination: the control of NF-κB activity. Ann Rev Immunol **18:** 621-663. *Ann Rev Immunol* **18**:621-663.

Kim YM, Lee BS, Yi KY, and Paik SG (1997) Upstream NF-kappaB site is required for the maximal expression of mouse inducible nitric oxide synthase gene in interferon-gamma plus lipopolysaccharide-induced RAW 264.7 macrophages. *Biochem Biophys Res Comm* **236**:655-660.

Lawrence T, Gilroy DW, Colville-Nash PR, and Willoughby DA (2001) Possible new role for NF-kB in the resolution of inflammation. *Nature Med* **7**:1291-1297.

Loewe R, Holnthoner W, Groger M, Pillinger M, Gruber F, Mechtcheriakova D, Hofer E, Wolff K, and Petzelbauer P (2002) Dimethylfumarate inhibits TNF-induced nuclear entry of NF-kappa B/p65 in human endothelial cells. *J Immunol* **168**:4781-4787.

Lyss G, Knorre A, Schmidt TJ, Pahl HL, and Merfort I (1998) The anti-inflammatory sesquiterpene lactone helenalin inhibits the transcription factor NF-kappaB by directly targeting p65. *J Biol Chem* **273**:33508-33516.

Manna SK, Sah NK, Newman RA, Cisneros A, and Aggarwal BB (2000) Oleandrin suppresses activation of nuclear transcription factor-kappaB, activator protein-1, and c-Jun NH2-terminal kinase. *Cancer Res* **60**:3838-3847.

Miyaji T, Hu X, Yuen PST, Muramatsu Y, Iyer S, Hewitt SM, and Star RA (2003) Ethyl pyruvate decreases sepsis-induced acute renal failure and multiple organ damage in aged mice. *Kidney Int* **64**:1620-1631.

Natarajan K, Singh S, Burke TR, Jr., Grunberger D, and Aggarwal BB (1996) Caffeic acid phenethyl ester is a potent and specific inhibitor of activation of nuclear transcription factor NF-kappa B. *Proc Natl Acad Sci USA* **93**:9090-9095.

O'Donnell-Tormey J, Nathan CF, Lanks K, DeBois CJ, and de la Harpe J (1987) Secretion of pyruvate. An antioxidant defense of mammalian cells. *J Exp Med* **165**:500-514.

Ruben SM, Dillon PJ, Schreck R, Henkel T, Chen CH, Maher M, Baeuerle PA, and Rosen CA (1991) Isolation of a rel-related human cDNA that potentially encodes the 65-kD subunit of NF-kappa B. *Science* **251**:1490-1493.

Rungeler P, Castro V, Mora G, Goren N, Vichnewski W, Pahl HL, Merfort I, and Schmidt TJ (1999) Inhibition of transcription factor NF-kappaB by sesquiterpene lactones: a proposed molecular mechanism of action. *Bioorg Med Chem* **7**:2343-2352.

Sappington PL, Fink ME, Yang R, Delude RL, and Fink MP (2003a) Ethyl pyruvate provides durable protection against inflammation-induced intestinal epithelial barrier dysfunction. *Shock* **20**:521-528.

Sappington PL, Han X, Yang R, Delude RL, and Fink MP (2003b) Ethyl pyruvate ameliorates intestinal epithelial barrier dysfunction in endotoxemic mice and immunostimulated Caco-2 enterocytic monolayers. *J Pharmacol Exp Ther* **304**:464-476.

Schmitz ML and Baeuerle PA (1991) The p65 subunit is responsible for the strong transcription activating potential of NF-kappa B. *EMBO J* **10**:3805-3817.

Schmitz ML, dos Santos Silva MA, and Baeuerle PA (1995) Transactivation domain 2 (TA2) of p65 NF-kappa B. Similarity to TA1 and phorbol ester-stimulated activity and phosphorylation in intact cells. *J Biol Chem* **270**:15576-15584.

Senftleben U and Karin M (2002) The IKK/NF-κB pathway. *Crit Care Med* **30**:S18-S26.

Sims CA, Wattanasirichaigoon S, Menconi MJ, Ajami AM, and Fink MP (2001) Ringer's ethyl pyruvate solution ameliorates ischemia/reperfusion-induced intestinal mucosal injury in rats. *Crit Care Med* **29**:1513-1518.

Song M, Kellum JA, Kaldas H, and Fink MP (2004) Evidence that glutathione depletion is a mechanism responsible for the anti-inflammatory effects of ethyl pyruvate in cultured lipopolysaccharide lipopolysaccharide-stimulated RAW 264.7 cells. *J Pharmacol Exp Ther* **308**:307-316.

Tak PP and Firestein GS (2001) NF-kappaB: a key role in inflammatory diseases. *J Clin Invest* **107**:7-11.

Tawadrous ZS, Delude RL, and Fink MP (2002) Resuscitation from hemorrhagic shock with Ringer's ethyl pyruvate solution improves survival and ameliorates intestinal mucosal hyperpermeability in rats. *Shock* **17**:473-477.

Toledano MB, Ghosh D, Trinh F, and Leonard WJ (1993) N-terminal DNA-binding domains contribute to differential DNA-binding specificities of NF-kappa B p50 and p65. *Mol Cell Biol* **13**:852-860.

Toledano MB and Leonard WJ (1991) Modulation of transcription factor NF-kappa B binding activity by oxidation-reduction in vitro. *Proc Natl Acad Sci USA* **88**:4328-4332.

Uchiyama T, Delude RL, and Fink MP (2003) Dose-dependent effects of ethyl pyruvate in mice subjected to mesenteric ischemia and reperfusion. *Intensive Care Med* **29**:2050-2058.

Ulloa L, Ochani M, Yang H, Halperin D, Yang R, Czura CJ, Fink MP, and Tracey KJ (2002) Ethyl pyruvate prevents lethality in mice with established lethal sepsis and systemic inflammation. *Proc Natl Acad Sci USA* **99**:12351-12356.

Venkataraman R, Kellum JA, Song M, and Fink MP (2002) Resuscitation with Ringer's ethyl pyruvate solution prolongs survival and modulates plasma cytokine and nitrite/nitrate concentrations in a rat model of lipopolysaccharide-induced shock. *Shock* **18**:507-512.

Yang R, Gallo DJ, Baust JJ, Uchiyama T, Watkins SK, Delude RL, and Fink MP (2002) Ethyl pyruvate modulates inflammatory gene expression in mice subjected to hemorrhagic shock. *Am J Physiol Gastrointest Liver Physiol* **283**:G212-G22.

Yang R, Han X, Delude RL, and Fink MP (2003) Ethyl pyruvate ameliorates acute alcohol-induced liver injury and inflammation in mice. *J Lab Clin Med* **142**:322-331.

Yang R, Uchiyama T, Alber SM, Han X, Watkins SK, Delude RL, and Fink MP (2004) Ethyl pyruvate ameliorates distant organ injury in a murine model of acute necrotizing pancreatitis. *Crit Care Med* **32**:1453-1459.

Footnotes:

*This work was funded by National Institutes of Health grant GM37631.

Figure Legends

Fig. 1. Effect of ethyl pyruvate on the expression iNOS mRNA in lipopolysaccharide-stimulated RAW cells. RAW cells were pretreated with the indicated concentrations of ethyl pyruvate for 30 min, and then incubated with or without lipopolysaccharide (100 ng/ml). Twenty four h later, total RNA was isolated and analyzed using semiquantitative RT-PCR. The depicted gel is representative of results that were obtained in an experiment that was repeated three times.

Fig. 2. Effect of ethyl pyruvate on iNOS protein expression in lipopolysaccharide-stimulated RAW cells. RAW cells were pretreated with the indicated concentrations of ethyl pyruvate for 30 min, and then incubated with or without lipopolysaccharide (100 ng/ml). After 24 h, total protein was extracted and analyzed by Western blot. The depicted gel is representative of results that were obtained in an experiment that was repeated three times.

Fig. 3. Effect of EA on NF-κB-dependent transcription in RAW cells. RAW cells were transiently cotransfected with 2 μg of pNF-κB-luc and 0.4 μg of pSV-β-galactosidase. Twenty-four h later, the cells were pretreated for 30 min with the indicated concentrations of ethyl pyruvate and then incubated in the absence or presence of lipopolysaccharide (100 ng/ml) for 30 min. Luciferase activity was determined and normalized to β-galactosidase activity (n=3 per condition). * indicates $P<0.05$ versus control; † indicates $P<0.05$ versus lipopolysaccharide in the absence of ethyl pyruvate.

Fig. 4. Effect of ethyl pyruvate on lipopolysaccharide-induced NF-κB DNA binding in RAW264.7 cells. For the gel depicted in Panel A, the cells were preincubated in the absence or presence of graded concentrations of ethyl pyruvate for 1 h, and then incubated in the absence or

presence of lipopolysaccharide (100 ng/ml) for 15 min. Nuclear extracts were prepared and EMSA was performed as described in the Materials and Methods section. To verify the identity of the NF-κB band detected by the EMSA, supershift assays using antibodies against the p65 and p50 subunits of NF-κB were performed as described in the Materials and Methods section (Panel B). Additionally, cold competition experiments were carried out, using a 100-fold molar excess of either unlabeled (specific) NF-κB duplex oligonucleotide or unlabeled (nonspecific) NF-IL6 duplex oligonucleotide (Panel B). The arrow indicates the NF-κB DNA complex. The gel depicted in Panel A is representative of results that were obtained in an experiment that was repeated three times. The gel depicted in Panel B is representative of results that were obtained in an experiment that was repeated twice.

Fig. 5. Effect of ethyl pyruvate on IκBα and IκBβ degradation in lipopolysaccharide-stimulated RAW264.7 cells. The cells were incubated with or without lipopolysaccharide (100 ng/ml) in the presence of the indicated concentrations of ethyl pyruvate. After incubation for 1 h, whole cell lysates were prepared, and Western blots analyzed. Western blotting for β-actin was used to verify equal loading. The depicted gel is representative of results that were obtained in an experiment that was repeated three times.

Fig. 6. Effects of ethyl pyruvate on basal NF-κB DNA-binding in unstimulated RAW264.7 cells. The cells were preincubated in the absence or presence of graded concentrations of ethyl pyruvate for 4 h. Then, nuclear extracts were prepared and EMSA was performed as described in the Materials and Methods section. Film was exposed for three days with an intensifying

screen. The arrow indicates the NF-κB DNA complex. The depicted gel is representative of results that were obtained in an experiment that was repeated twice.

Fig. 7. Effects of ethyl pyruvate on DNA binding by detergent-activated NF-κB. RAW 264.7 cells were preincubated in the absence or presence of graded concentrations of ethyl pyruvate for 2 h. Cytoplasmic fractions were prepared as described in the Material and Methods section, and dialyzed against 10,000 volumes of buffer II. The extracts were adjusted to 0.2 % deoxycholate (v/v), incubated on ice for 15 min, supplemented with Nonidet P-40 to 0.2 % (v/v), and then incubated for an additional 15 min on ice before subjecting them to EMSA. The arrow indicates the NF-κB DNA complex. The depicted gel is representative of results that were obtained in an experiment that was repeated four times.

Fig. 8. Effect of ethyl pyruvate on DNA binding by recombinant human p50 homodimers. Eleven ng of human recombinant p50 was incubated with the indicated concentrations of ethyl pyruvate at 37 °C for 2 h. Binding buffer and poly(dI·dC) were then added, and the samples assayed for DNA binding as described in the Materials and Methods. The depicted gel is representative of results that were obtained in an experiment that was repeated three times.

Fig. 9. Effect of ethyl pyruvate on DNA binding by wt-p65 homodimers. 293 cells were transiently transfected with 2 μg of a wt-p65 expression vector (lane 2-6), or Rc/CMV control vector (lane 1). Twenty-four h after transfection, the cells were incubated in the absence or presence of graded concentrations of ethyl pyruvate for 4 h, as indicated. Total cell extracts were prepared and analyzed for NF-κB DNA binding by EMSA (Panel A). To verify the identity of

the NF-κB band detected by the EMSA, supershift assays using antibodies against the p65 and p50 subunits of NF-κB were carried out (Panel B). Additionally, cold competition experiments were performed, using a 100-fold molar excess of either unlabeled (specific) NF-κB duplex oligonucleotide or unlabeled (nonspecific) NF-IL6 duplex oligonucleotide (Panel B). The arrow indicates the NF-κB DNA complex. The gel depicted in Panel A is representative of results that were obtained in an experiment that was repeated three times. The gel depicted in Panel B is representative of results that were obtained in an experiment that was repeated twice.

Fig. 10. Effect of ethyl pyruvate on DNA binding by Cys^{38}/p65 homodimers. 293 cells were transiently transfected with 2 μg of a Cyc^{38}/p65 expression vector (lane 2-6), or Rc/CMV control vector (lane 1). Twenty-four h after transfection, the cells were incubated in the absence or presence of graded concentrations of ethyl pyruvate for 4 h, as indicated. Total cell extracts were prepared and analyzed for NF-κB DNA binding by EMSA. The arrow indicates the NF-κB DNA complex. The depicted gel is representative of results that were obtained in an experiment that was repeated three times.

Fig. 11. Effect of ethyl pyruvate on DNA binding by Cys^{120}/p65 homodimers. 293 cells were transiently transfected with 2 μg of a Cys^{120}/p65 expression vector (lane 2-6), or Rc/CMV control vector (lane 1). Twenty-four h after transfection, the cells were incubated in the absence or presence of graded concentrations of ethyl pyruvate for 4 h, as indicated. Total cell extracts were prepared and analyzed for NF-κB DNA binding by EMSA. The arrow indicates the NF-κB

DNA complex. The depicted gel is representative of results that were obtained in an experiment that was repeated three times.

JPET Fast Forward. Published on November 3, 2004 as DOI: 10.1124/jpet.104.079707
This article has not been copyedited and formatted. The final version may differ from this version.

Figure 1

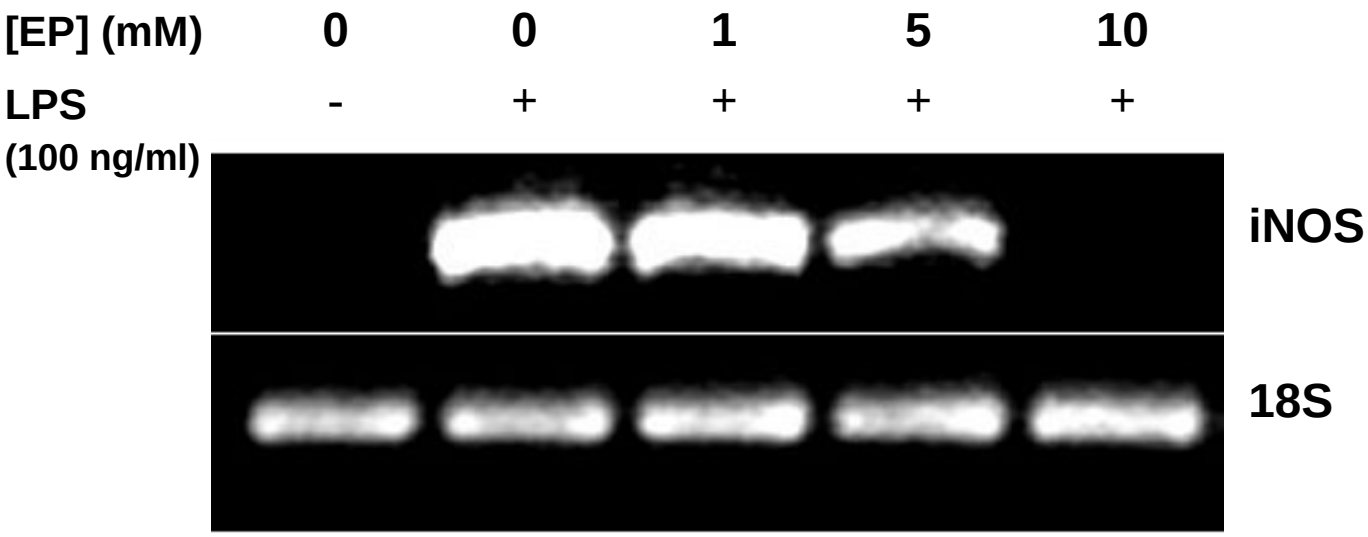

JPET Fast Forward. Published on November 3, 2004 as DOI: 10.1124/jpet.104.079707
This article has not been copyedited and formatted. The final version may differ from this version.

Figure 2

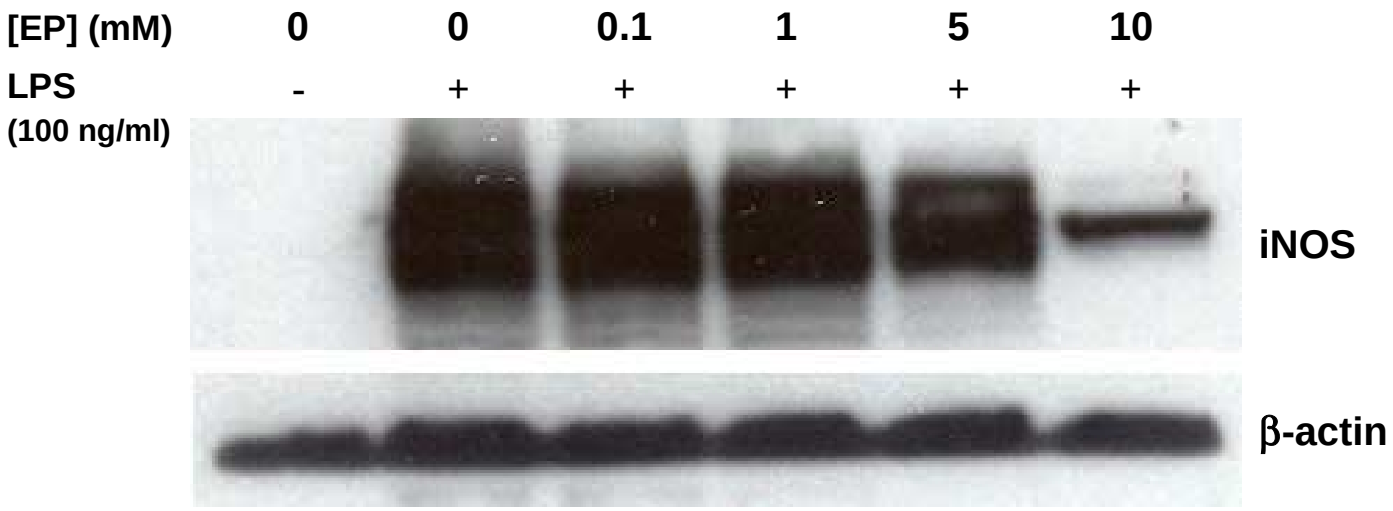

JPET Fast Forward. Published on November 3, 2004 as DOI: 10.1124/jpet.104.079707
This article has not been copyedited and formatted. The final version may differ from this version.

Figure 3

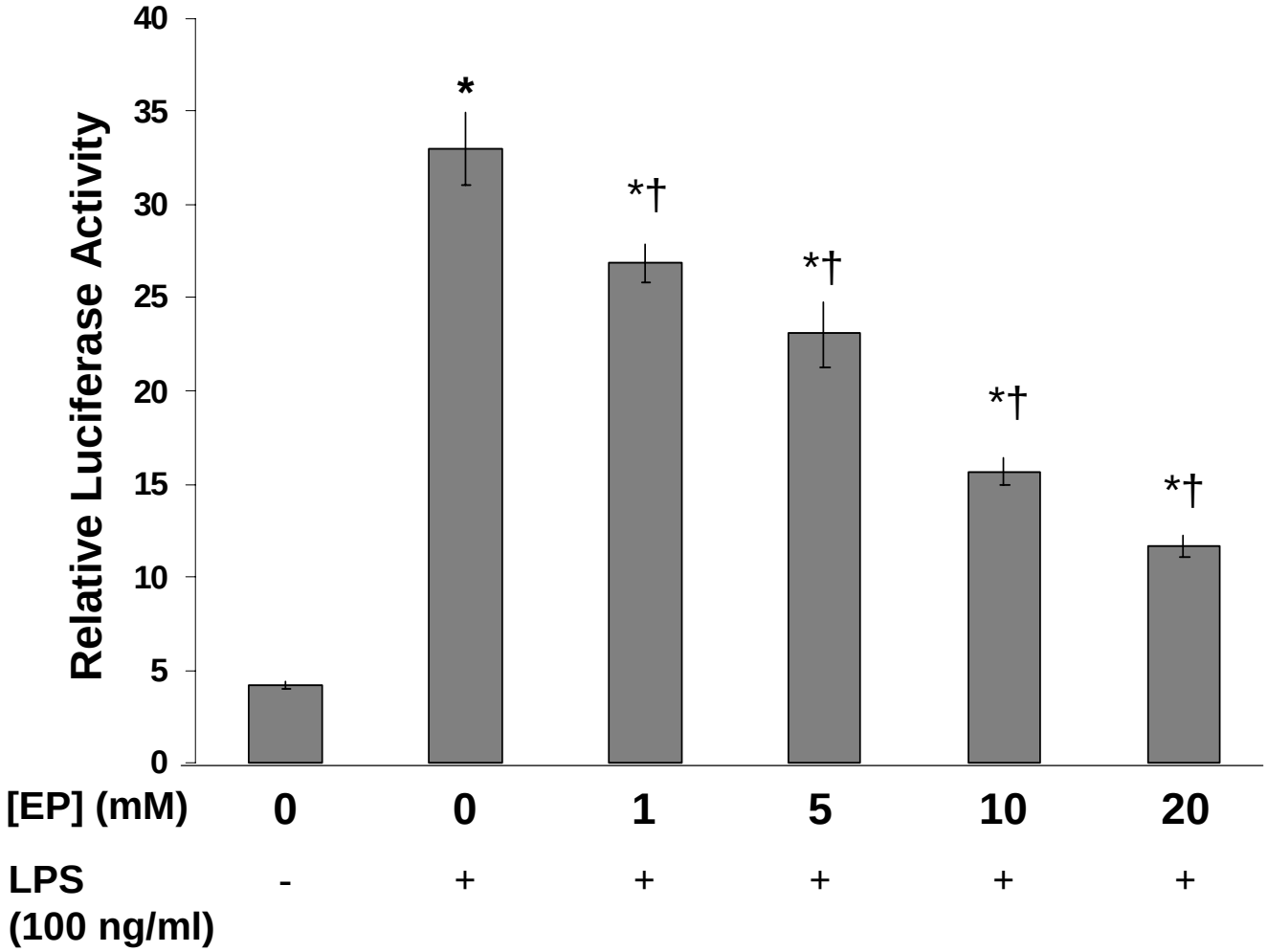

JPET Fast Forward. Published on November 3, 2004 as DOI: 10.1124/jpet.104.079707
This article has not been copyedited and formatted. The final version may differ from this version.

Figure 4

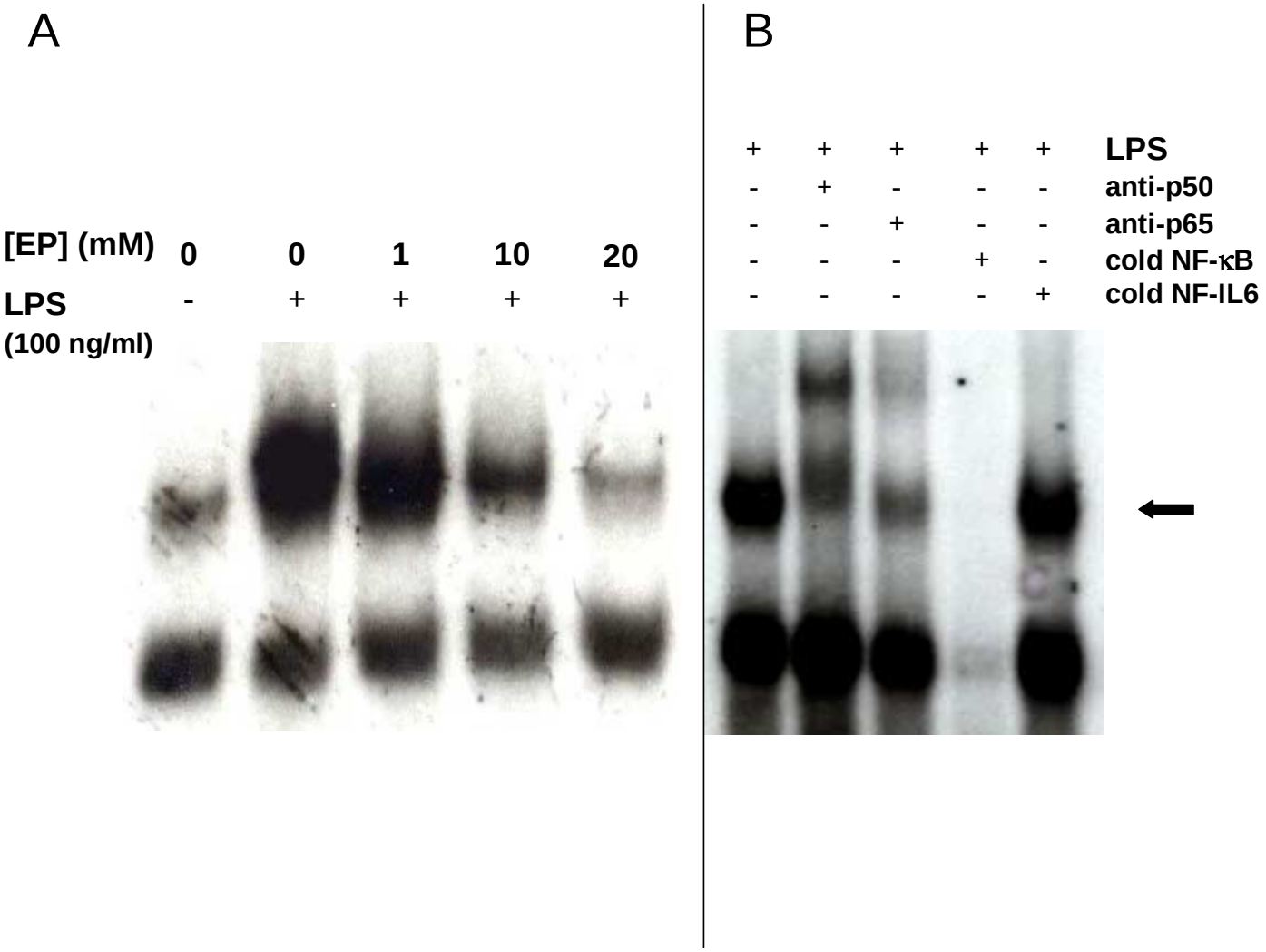

JPET Fast Forward. Published on November 3, 2004 as DOI: 10.1124/jpet.104.079707
This article has not been copyedited and formatted. The final version may differ from this version.

Figure 5

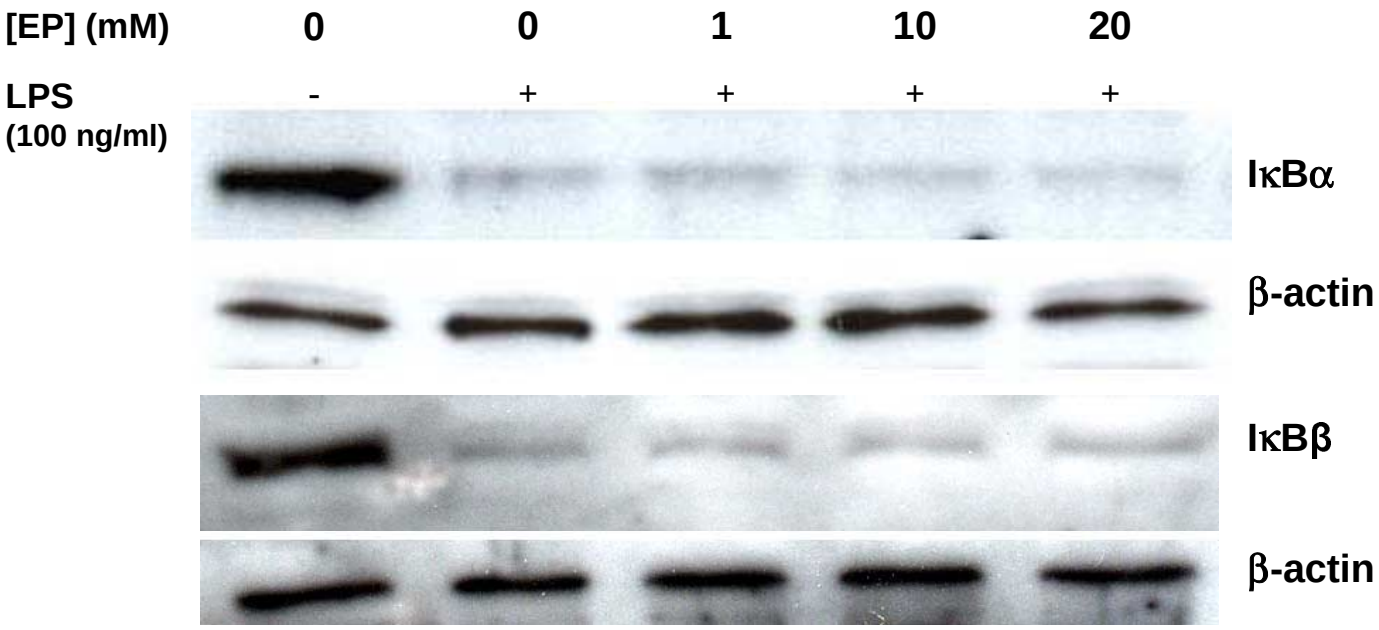

JPET Fast Forward. Published on November 3, 2004 as DOI: 10.1124/jpet.104.079707
This article has not been copyedited and formatted. The final version may differ from this version.

Figure 6

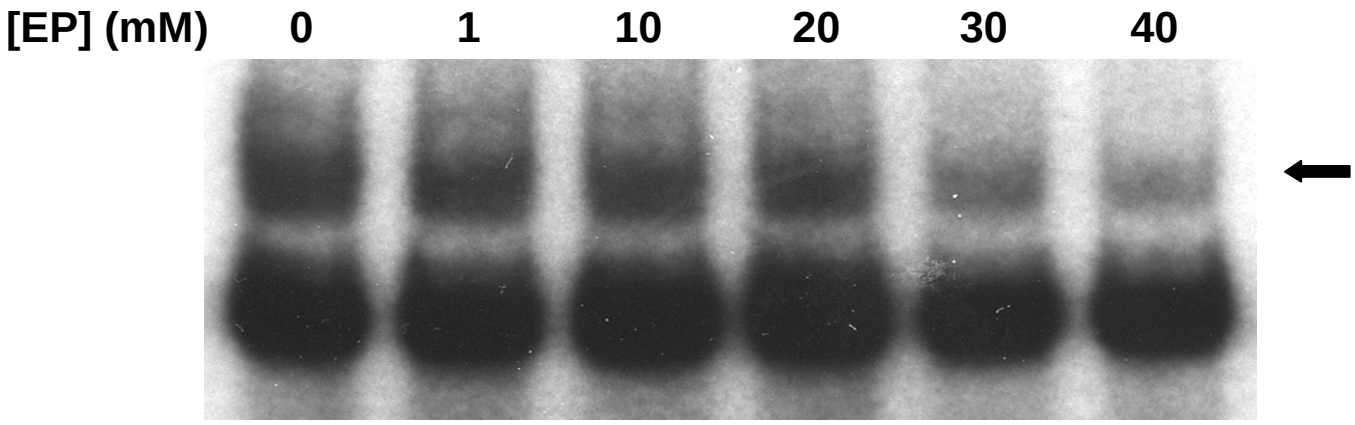

JPET Fast Forward. Published on November 3, 2004 as DOI: 10.1124/jpet.104.079707
This article has not been copyedited and formatted. The final version may differ from this version.

Figure 7

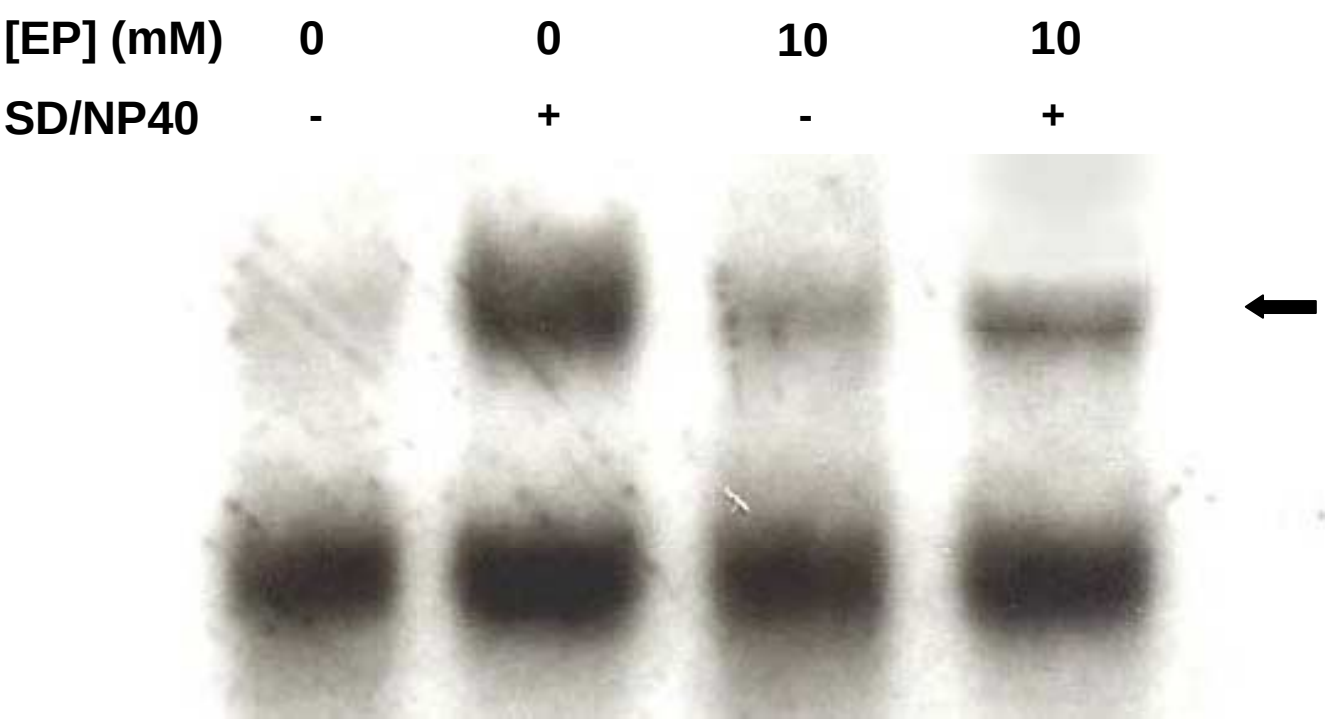

JPET Fast Forward. Published on November 3, 2004 as DOI: 10.1124/jpet.104.079707
This article has not been copyedited and formatted. The final version may differ from this version.

Figure 8

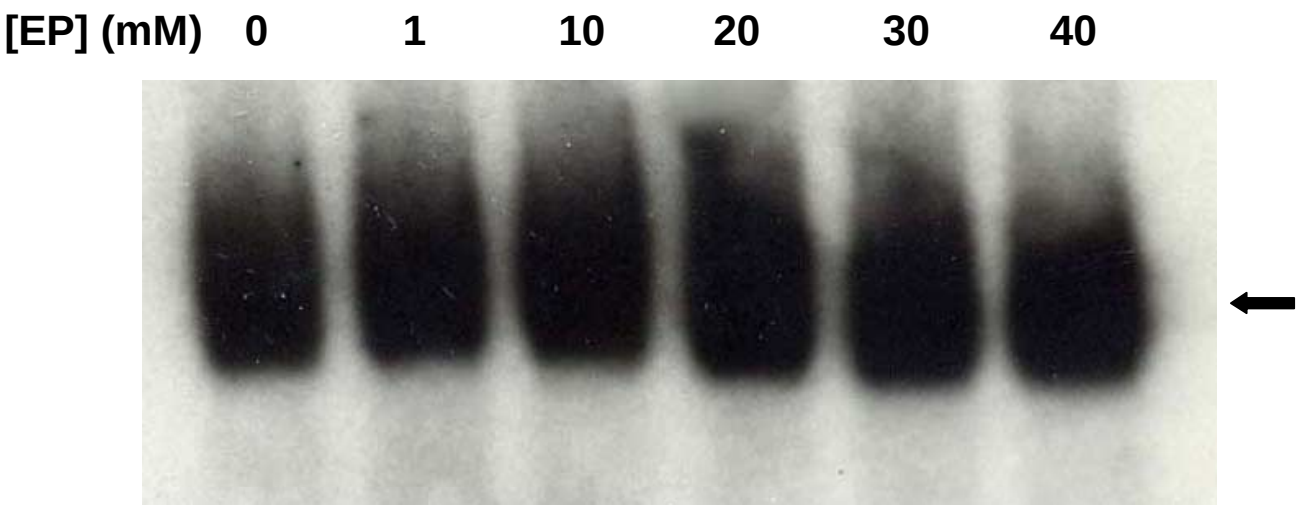

JPET Fast Forward. Published on November 3, 2004 as DOI: 10.1124/jpet.104.079707
This article has not been copyedited and formatted. The final version may differ from this version.

Figure 9

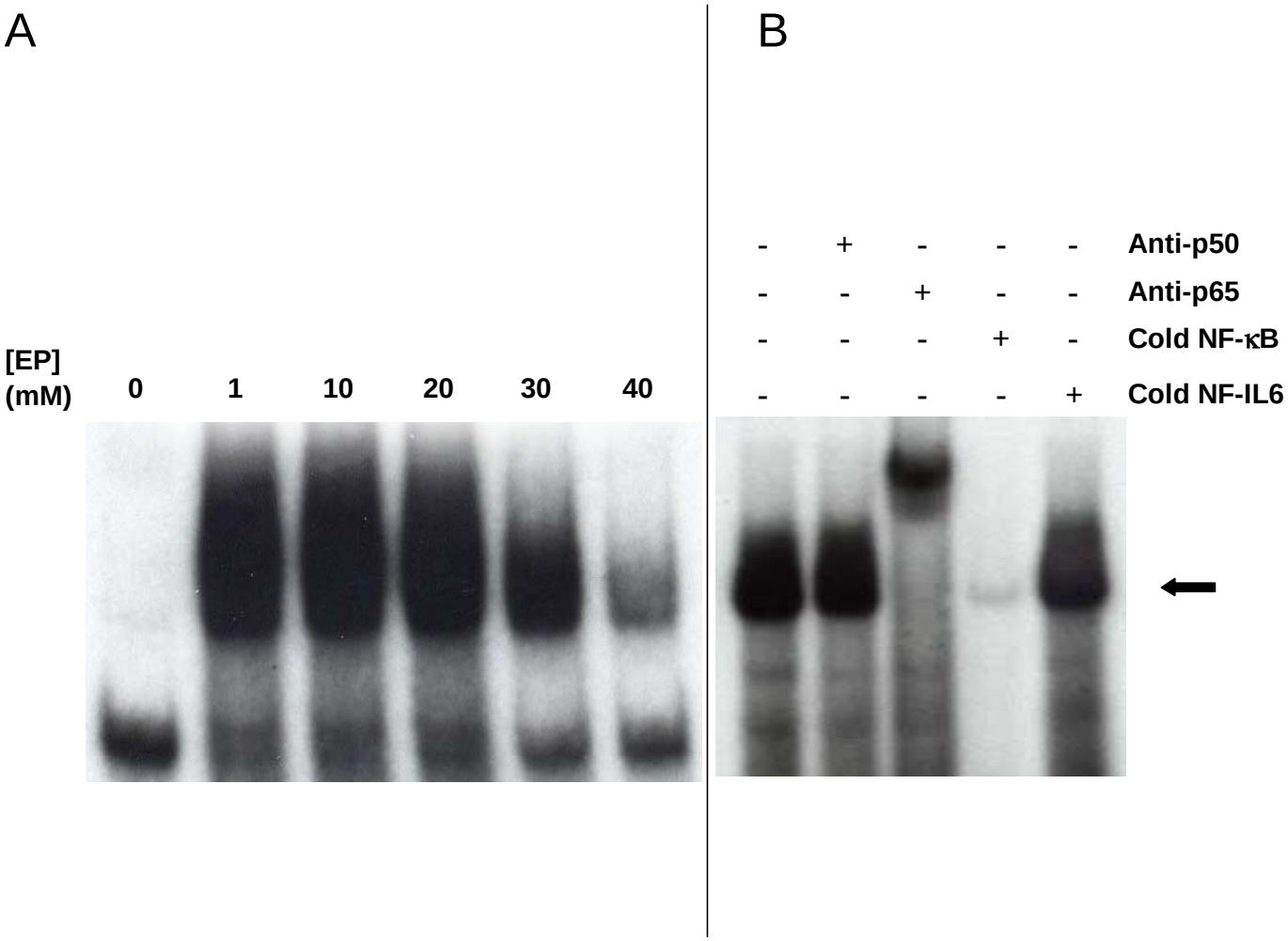

JPET Fast Forward. Published on November 3, 2004 as DOI: 10.1124/jpet.104.079707
This article has not been copyedited and formatted. The final version may differ from this version.

Figure 10

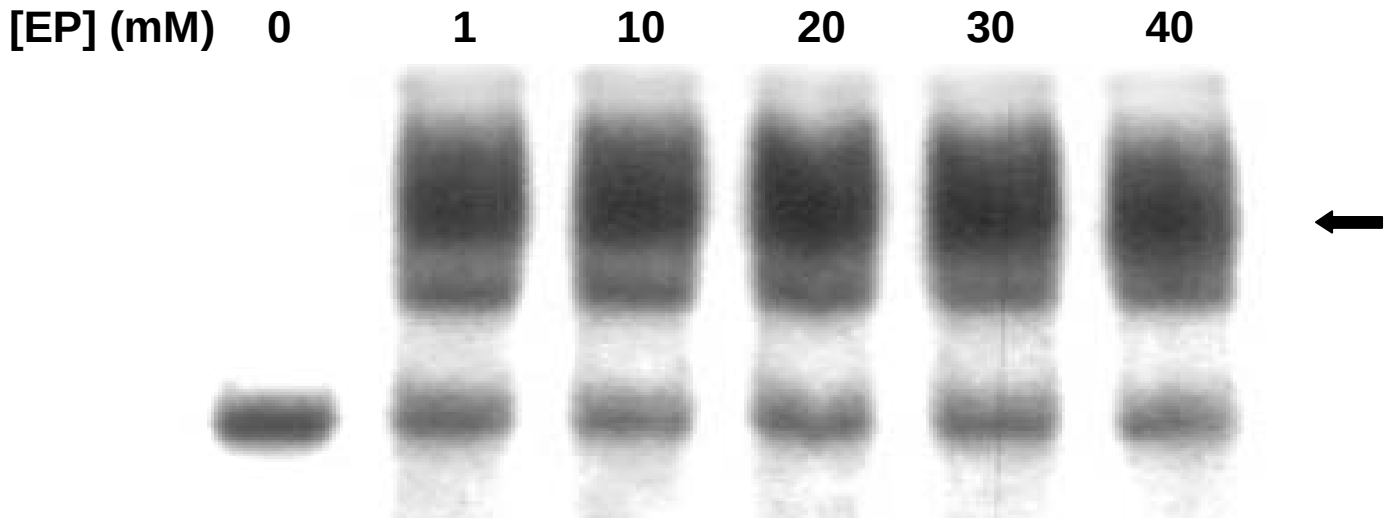

JPET Fast Forward. Published on November 3, 2004 as DOI: 10.1124/jpet.104.079707
This article has not been copyedited and formatted. The final version may differ from this version.

Figure 11